Progress in Natural Science: Materials International xxx (xxxx) xxx–xxx

HOSTED BY

ELSEVIER

Contents lists available at ScienceDirect

Progress in Natural Science: Materials International

journal homepage: www.elsevier.com/locate/pnsmi

Original Research

Multiscale structures of Zr-based binary metallic glasses and the correlation with glass forming ability☆

Xuelian Wu[a], Si Lan[a,b], Zhenduo Wu[a,c], Xiaoya Wei[a,c], Yang Ren[d], Ho Yin Tsang[a], Xunli Wang[a,c,*]

[a] Department of Physics, City University of Hong Kong, 83 Tat Chee Avenue, Kowloon, Hong Kong, China
[b] Herbert Gleiter Institute of Nanoscience, School of Materials Science and Engineering, Nanjing University of Science and Technology, 200 Xiaolingwei, Xuanwu District, Nanjing, China
[c] Center of Neutron Scattering, City University of Hong Kong Shenzhen Research Institute, 8 Yuexing 1st Road, Shenzhen Hi-Tech Industrial Park, Nanshan District, Shenzhen 518057, China
[d] X-ray Science Division, Argonne National Laboratory, 9700 S. Cass Avenue, Argonne, IL 60439, USA

ARTICLE INFO

Keywords:
Metallic glasses
Glass forming ability
Densely atomic packing
Nanoscale inhomogeneity
Crystallization

ABSTRACT

Thermal behaviors and structures of three Zr-based binary glass formers, $Zr_{50}Cu_{50}$, $Zr_{64}Cu_{36}$ and $Zr_{64}Ni_{36}$, were investigated and compared using differential scanning calorimetry (DSC), transmission electron microscopy (TEM), high energy X-ray diffraction (XRD) and small angle X-ray scattering (SAXS). The high energy XRD results show that the bulk glass former $Zr_{50}Cu_{50}$ has a denser atomic packing efficiency and reduced medium-range order than those of marginal glass formers $Zr_{64}Cu_{36}$ and $Zr_{64}Ni_{36}$. Based on TEM observations for the samples after heat treatment at 10 K above their crystallization onset temperatures, the number density of crystals for $Zr_{50}Cu_{50}$ was estimated to be 10^{23}–10^{24} m^{-3}, which was four-orders higher than that in $Zr_{64}Cu_{36}$ and $Zr_{64}Ni_{36}$ metallic glasses. SAXS results indicate that $Zr_{50}Cu_{50}$ has higher degree of nanoscale inhomogeneities than those in $Zr_{64}Cu_{36}$ and $Zr_{64}Ni_{36}$ at as-cast state. The observed multiscale structures are discussed in terms of the phase stability and glass-forming ability of Zr-based binary glass formers.

1. Introduction

Metallic glasses (MGs) are formed by quenching metallic liquids to suppress crystallization [1]. It is challenging to probe the microstructure of MGs using microscopy due to artifacts induced during sample preparation [2]. Over the past decades, scattering experiments and simulations were performed to study the structure of MGs [3–7] and to provide a link between the structure and the glass formation. Short-range order (SRO) was believed to play an important role on formation of MGs upon cooling [8,9]. It was found recently that atomic re-arrangement and re-ordering at medium range scale contribute prominently to the connectivity and further densely packing for MGs [10–12].

Recently, it was proposed that MGs contain nanoscale inhomogeneous structure [13–16] beyond medium-range length scale which results in unique properties and also has a possible correlation with glass forming ability (GFA). However, the structural origin for the correlation is still unclear. Most recently, Lan et al. [17] observed a large amount of density fluctuations at nanoscale in a good ternary glass former $Zr_{46}Cu_{46}Al_8$ before crystallization using in-situ techniques. The nanoscale heterogeneous structures may link the unique crystallization behavior to the GFA in $Zr_{46}Cu_{46}Al_8$. Here, we studied atomic-to-nanoscale structures of three binary alloys, $Zr_{50}Cu_{50}$, $Zr_{64}Cu_{36}$ and $Zr_{64}Ni_{36}$, and tried to correlate the structures with GFA. These systems are chosen because of their simple chemistry and different GFAs. We observed a different crystallization behavior of a bulk binary glass former $Zr_{50}Cu_{50}$ comparing with two marginal glass formers $Zr_{64}Cu_{36}$ and $Zr_{64}Ni_{36}$. Multi-length scale characterization techniques were employed, including high energy X-ray diffraction (XRD) for atomic structure studies, e.g. atomic packing efficiency [18] and nearest neighbors using pair distribution function (PDF) analysis, small angle X-ray scattering (SAXS) for probing the density fluctuations at nanoscale.

2. Experimental methods

Glassy ribbons of $Zr_{50}Cu_{50}$, $Zr_{64}Cu_{36}$ and $Zr_{64}Ni_{36}$ (at. %) were fabricated by melt spinning with a wheel speed of ~ 30 m/s. The

☆ Peer review under responsibility of Chinese Materials Research Society.

* Corresponding author at: Department of Physics, City University of Hong Kong, 83 Tat Chee Avenue, Kowloon, Hong Kong, China.
E-mail address: xlwang@cityu.edu.hk (X. Wang).

http://dx.doi.org/10.1016/j.pnsc.2017.08.008
Received 19 December 2016; Received in revised form 13 August 2017; Accepted 16 August 2017

amorphous structure of as-spun samples was confirmed by wide angle X-ray scattering using a SAXSpace with Mo K_α radiation (Anton Paar, Graz, Austria), high energy XRD, and transmission electron microscope (TEM) (Phillips CM20 FEG).

The thermal stability of the amorphous as-spun ribbons was studied by a Perkin Elmer differential scanning calorimeter (DSC-7) at a constant heating rate of 10 K/min under flowing nitrogen. The glass transition temperature T_g and the crystallization temperature T_x were determined as the onsets of each event, using the two-tangents method. High energy XRD experiments were conducted at the beamline 11-ID-C, Advanced Photon Source, Argonne National Laboratory. The wavelength of the X-ray is 0.11798 Å. The diffraction spectra were acquired in transmission geometry by a 2D detector. To reduce the noise, the 2D images were azimuthally integrated. The structure factor S(Q) was obtained after the correction of detector efficiency, background scattering, polarization, absorption, and Compton scattering. The reduced pair distribution function (PDF), G(r), is obtained from the Fourier transform of S(Q): $G(r) = (2/\pi) \times \int_0^{Q_{max}} Q(S(Q)-1)\, sin(Qr) dQ$, where r is the distance in real space and $Q = 4\pi sin\theta/\lambda$. Here θ is half of the scattering angle between the incident beam and the scattered beam. λ is the X-ray wavelength.

Three MGs, were heated to the temperature ~ 10 K above T_x at a heating rate of 10 K/min in nitrogen atmosphere. They were subsequently cooled back to ambient temperature (cooling rate ~ 200 K/min). The MGs after above heat treatment in DSC were examined by TEM. The TEM foils were prepared by ion milling using a Gatan precision ion mill (PIPS) with the argon ion beam energy ~ 3 keV and the incident angle 5°. Amorphous and crystallized samples were also studied by SAXS. Thin foils with 30 μm thickness were polished for SAXS. Room temperature SAXS measurements were performed on the SAXSpace line collimation camera. The sample chamber was evacuated to vacuum during measurements to reduce the background noise. The scattering patterns were acquired in transmission geometry by a 2D detector. The 2D images were integrated azimuthally, corrected for background scattering and normalized using SAXStreat and SAXSquant software supplied by the vendor (Anton Paar). The resulting scattering intensity I(Q) was plotted as a function of the scattering vector Q.

3. Results and discussion

Fig. 1 shows the DSC traces of melt-spun Zr-Cu and Zr-Ni binary MGs conducted at a constant heating rate of 10 K/min. The glass transition and crystallization onset temperatures are marked as T_g

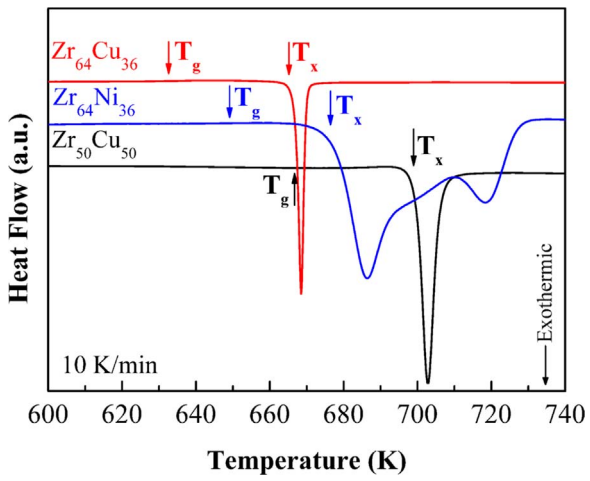

Fig. 1. DSC traces of as-spun Zr-Cu and Zr-Ni binary MGs conducted at a heating rate of 10 K/min. The glass transition temperature T_g can be referred to literatures [19,20,23] and the crystallization temperature T_x were determined as the onsets of the respective events using the two-tangents method, which are all arrowed in patterns.

Table 1
Thermophysical parameters of Zr-based binary metallic glasses.

Compositions	T_g (K)	T_x (K)	T_l (K)	T_{rg}	γ
$Zr_{50}Cu_{50}$	667	701	1226	0.544	0.370
$Zr_{64}Cu_{36}$	632	665	1284	0.492	0.347
$Zr_{64}Ni_{36}$	649	676	1283	0.506	0.350

and T_x respectively. For the Zr-Cu amorphous alloys, when the Cu content increases from 36% to 50%, T_g [19,20] increases from 632 K to 667 K. There is a similar trend for their T_x in accordance with the previous results [19,21,22]. For eutectic $Zr_{64}Ni_{36}$ alloy, T_g [23] is about 649 K. The characteristic temperatures T_g, T_x and T_l [24,25] are summarized in Table 1. From the above results, the common GFA criteria such as $\gamma = T_x / (T_g + T_l)$ [26] and $T_{rg} = T_g / T_l$ [27] parameters were evaluated. It clearly shows that the γ and T_{rg} of $Zr_{50}Cu_{50}$ are significantly higher than the corresponding values of the other two glasses, indicating a better GFA of $Zr_{50}Cu_{50}$ alloy. This is consistent with the experimental results [28–30] that $Zr_{50}Cu_{50}$ is a bulk glass former while $Zr_{64}Ni_{36}$ and $Zr_{64}Cu_{36}$ can only be made in ribbon shape. In addition, the γ and T_{rg} of $Zr_{64}Ni_{36}$ are slightly higher than that of $Zr_{64}Cu_{36}$, implying a better GFA of $Zr_{64}Ni_{36}$ than $Zr_{64}Cu_{34}$.

The crystallized samples were prepared by the heat treatment as described in the experimental part. Their microstructures were studied by TEM. Fig. 2(a)-(c) shows the TEM bright filed (BF) images of the crystallized $Zr_{50}Cu_{50}$, $Zr_{64}Cu_{36}$, and $Zr_{64}Ni_{36}$. The insets of Fig. 2(a)-(c) are the corresponding selected area electron diffraction (SAED) patterns. For $Zr_{50}Cu_{50}$, the SAED has only several sharp rings. No obvious diffraction spots are found, indicating the existence of a finely dispersed nanocrystals with random orientations. The BF image further confirms that there are a lot of black and grey crystalline spherical particles embedded in the amorphous matrix. In addition, the size distribution of the nanoscale crystalline particles determined from the BF image is shown in Fig. 2(d). From Fig. 2(d), the mean crystalline particle size is found to be about 16.0 nm. In $Zr_{64}Ni_{36}$, however, several bright diffraction spots are found in SAED, indicating there exist a small amount of crystals with large size. The corresponding BF image also confirms that the crystal size is large (~ 200 nm) and the amount is small. In $Zr_{64}Cu_{36}$, the diffraction spots are even sharper than those of the $Zr_{64}Ni_{36}$. Interestingly, large black areas ~ 100 nm (as indicated by the red dashed lines in Fig. 2(b) in the crystalline precipitates) can be observed, which is consistent with the clear diffraction spots in the SAED. The BF image and SAED of crystalline $Zr_{64}Cu_{36}$ alloy illustrated that the crystals can grow very large and can maintain the same crystal orientation.

The crystallized $Zr_{50}Cu_{50}$ was then studied by SAXS and the resulting I(Q) is shown in Fig. 3(a). From TEM observation, the crystalline particles are roughly in a spherical shape. The real space pair distance distribution function p(r) or PDDF can be obtained by the equation $p(r) = (1/2\pi^2) \times \int_0^\infty I(Q) Qr sin(Qr) dQ$ [31]. Fig. 3(b) shows the p(r) of crystalline particles obtained by the indirect Fourier transformation of I(Q) using GIFT (Anton Paar). The average diameter of nanocrystals in $Zr_{50}Cu_{50}$ is found to be ~ 18 nm, which agrees well with the size determined by TEM.

According to the TEM and SAXS results, the estimated diameter of a crystal in $Zr_{50}Cu_{50}$ is about 16–18 nm. By calculation, the crystal's volume $V_{crystal}$ is about 2×10^3 nm^3. Thus, for a fully crystallized $Zr_{50}Cu_{50}$, the number density of crystals can be estimated by $1/V_{crystal}$, which is about 10^{23}–10^{24} m^{-3}. This is 4 orders higher than the estimated crystal number density in the crystallized $Zr_{64}Cu_{36}$ and $Zr_{64}Ni_{36}$. Since all three MGs were prepared by similar methods, the significant increase of crystal density should not come from the quenched-in impurities. What's